Coherent pulse propagation in a resonant absorber with Kerr-type nonlinearity

Ljubomir Matulic,* G. E. Torres-Cisneros,† and J. J. Sanchez-Mondragón

Centro de Investigaciones en Optica, A.C., Departamento de Optica Cuántica y Láseres, Apartado Postal 948, Léon, Guanajuato, México, 37000

Received February 6, 1990; revised manuscript received October 22, 1990; accepted January 10, 1991

We present a numerical study of the non-steady-state pulse propagation in a resonant inhomogeneously broadened absorber embedded in a dielectric medium with a Kerr-type nonlinearity. We find that the individual atomic dipoles are dephased and that their evolution depends on their detunings. We think that this is the reason for small energy losses that prevent the pulse from attaining a truly steady-state nature. We discuss the implications of this result in relation to previous studies. Our results point to the existence of near-steady-state Kerr pulses, similar to the ideal solitons.

1. INTRODUCTION

Steady-state pulses are an expected feature of most nonlinear propagation problems because of the ability of the nonlinearities to cancel out the linear dispersion and hence the pulse absorption. This feature is common to pulse propagation in passive as well as resonant media. In each case there is a theoretical and experimental framework that predicts the existence of solitons. However, the problem of propagation in a medium with both nonlinearities is a different matter. Steady-state propagation in this setting has been suspected for a long time, but the experimental evidence is insufficient and limited, while the development of its theory is hampered by an inability to apply previously successful analytic methods.

Within this class of problems is pulse propagation in the presence of the optical Kerr effect, a nonlinear and nonresonant phenomenon that has proved to be of great interest in theoretical and experimental research on pulse propagation through different absorbing and amplifying media. The Kerr effect is a passive nonlinearity that turns out to be a source of, among other things, phase modulation or chirping and the existence of stationary pulses in nonresonant media like optical fibers. As first shown by Hasegawa and Tappert,[1] the phase modulation produced by the Kerr nonlinearity may counteract the dispersive effects inherent in the fiber, permitting the propagation through the fiber of undistorted light pulses. Among the most interesting practical applications of this fact are the compression of pulses to temporal widths of only a few femtoseconds[2] and the elegant proposal of a so-called soliton laser.[3]

On the other hand, as first shown by Eberly and Matulic,[4,5] the inclusion of the Kerr effect in a resonant medium with a homogeneously broadened atomic line leads to the possibility of pulse propagation of self-induced transparency- (SIT-) type pulses.[6] However, we, as well as some other workers,[7] were unable to obtain a self-consistent analytic solution for the more realistic case of an inhomogeneously broadened atomic line in which the distribution of transition frequencies is comparable to or larger than the spectral width of the pulse. We have recently published some numerical results for the steady-state pulse propagation in broad-line absorbers in the presence of a Kerr nonlinearity.[8] There, we assumed the existence of the steady-state pulses in the presence of a Kerr nonlinearity and solved numerically the corresponding steady-state equations. Then we showed that such pulses exist, that they possess an asymmetric chirp, and that they are not factorable. We ascribed to this last-named fact the impossibility of finding analytic solutions to this problem.

In the present paper we abandon the *a priori* assumption of the existence of steady-state solutions and examine the problem from a more physically realistic point of view; i.e., we study the way in which the pulse actually propagates in the resonant Kerr medium and whether it eventually evolves toward the steady state. One of the most important results that we have found is that the Kerr pulse never achieves a truly steady state. Its area seems to remain stable, but its energy shows a small but unmistakable decay. This fact disqualifies the Kerr pulse from being considered a true soliton. We have found that this small loss of energy is associated with the behavior of the microscopic absorptive components of the atomic polarization. They show a quite pronounced dephasing; i.e., their temporal evolution is strongly dependent on detuning. We think that this is the reason for the energy loss of the pulse.

As the Kerr nonlinearity or the atomic linewidth is decreased in magnitude, the dephasing of the absorptive components of the atomic polarization tends to disappear, so that at the limit of no Kerr nonlinearity and no Doppler broadening we recover the ideal soliton solutions.

Moreover, we think that the dephasing of the atomic polarizations is the reason for the breakdown of the factorization assumption. Since this assumption seems to be the only way to arrive at stable, shape-preserving, and energy-conserving pulses, we conclude not only that the factorization assumption is a mathematical ansatz but that it has an important physical content; that is, this factorability condition is intimately related to the existence of ideal solitons and ideal pulse trains.

0740-3224/91/061276-08$05.00

In our theory the departure of a Kerr pulse from an ideal soliton is so small that we are inclined to think of it as a quasi-steady-state structure, which a simple experiment would not be able to distinguish easily from a truly steady-state pulse.

2. NON-STEADY-STATE PULSE-MEDIUM DYNAMICS

In this section we present briefly the basic equations that govern the interaction between a light pulse and the resonant and nonresonant media in which it propagates. We describe this interaction in both the temporal and the frequency domains.

We consider a laser pulse with carrier angular frequency ω_L propagating through two-level inhomogeneously broadened resonant atoms embedded in a dielectric characterized by a Kerr-type nonlinearity. In the usual slowly varying envelope and phase approximation the pulse is given by

$$E(t,z) = \mathscr{E}(t,z)\exp[i(kz - \omega_L t)] + \text{c.c.}, \tag{1}$$

where $\mathscr{E}(t,z)$ is the slowly varying complex envelope of the electric field and k is its wave number. The interaction between the pulse and the medium can be described by the following set of partial integrodifferential equations, which we will refer to as the Kerr optical Bloch–Maxwell equations:

$$\partial p/\partial t = i(\Delta p + \hat{\Omega} w), \tag{2a}$$

$$\partial w/\partial t = \mathrm{Im}(\hat{\Omega} p^*), \tag{2b}$$

$$(\partial/\partial z + \partial/c_0\,\partial t)\hat{\Omega} = -i(B\langle p\rangle + C_K|\hat{\Omega}|^2\hat{\Omega}), \tag{2c}$$

where $p = u + iv$ is the complex envelope of the atomic polarization, w is the atomic inversion, $\Delta = \omega - \omega_L$ is the detuning of an individual atom's transition frequency ω from the laser's frequency ω_L, and $c_0 = c/\eta_0$ is the velocity of light in the dielectric. The transition frequencies are assumed to be distributed about the central frequency ω_L, and their distribution is assumed to be described by a normalized atomic line-shape function $g(\omega - \omega_L) = g(\Delta)$, whose bandwidth (FWHM) is denoted by $1/T_2^*$. Finally, the quantity Ω is referred to as the complex Rabi frequency and is defined by

$$\tilde{\Omega}(t,z) = \kappa\mathscr{E}(t,z) = (2d/\hbar)\mathscr{E}(t,z), \tag{3}$$

where d is the matrix element of the atomic dipole. The definition given in Eq. (3) is more suitable for numerical calculations than an equivalent definition more frequently used in analytic studies of pulse propagation[5]:

$$\hat{\Omega}(t,z) = \Omega(t,z)\exp(i\Phi), \tag{4a}$$

where

$$\Phi = \Delta k z - \Delta\omega_L t + \phi(t,z). \tag{4b}$$

Here Ω and ϕ are the real amplitude and the phase modulation of $\tilde{\Omega}$, respectively. In Eq. (4b) Δk and $\Delta\omega_L$ are the frequency and the wave-number pullings of the pulse, and they are defined as the linear terms in z and t of the phase modulation $\phi(t,z)$ of $\hat{\Omega}(t,z)$.

In Eq. (2c) the constant B, with dimensions in inverse centimeter-seconds, depends on the medium and is given by $B = 2a^2/\eta_0 c = \alpha/2\pi g(0)$, where η_0 is the linear part of the index of refraction of the passive dielectric, c is the velocity of light in vacuum, and $a^2 = (\pi/2)Nh\,\omega_L\kappa^2$, in which N is the number of active atoms per unit volume. The quantity α^{-1} is sometimes referred to as the cooperative time of the active medium, and α^{-1} is the Beer length. We will refer to B as the propagation constant.

The second constant that appears in Eq. (2c), with dimensions in (inverse centimeters) × (squared seconds), is given by $C_K = \beta\omega_L/c\kappa^2$, where β is the Kerr constant of the background dielectric, which defines its nonlinear index of refraction through the relation

$$\eta = \eta_0(1 + \beta\mathscr{E}^2). \tag{5}$$

We will call the constant C_K simply the Kerr constant.

Finally, the angle brackets in Eq. (2c) represent the averaging of the quantity enclosed within them with respect to the atomic line $g(\Delta)$.

Equation (2c) can be simplified if we make the following change of independent variables:

$$z' = z, \qquad t' = t - z/c_0. \tag{6}$$

The complex Rabi frequency $\hat{\Omega}$ of Eqs. (4) transforms into

$$\Omega(t',z) = \Omega(t',z)\exp\{i[\Delta k' z - \Delta\omega_L t' + \phi(t',z)]\}, \tag{7a}$$

where

$$\Delta k' = \Delta k - \Delta\omega/c_0 \tag{7b}$$

is the wave-vector pulling referred to the (z,t') frame. From Eqs. (6) it follows that

$$\partial/\partial z + \partial/c_0\partial t = \partial/\partial z', \tag{8}$$

and the Maxwell equation for $\Omega(t',z)$ [Eq. (2c)] can now be written as

$$\partial\hat{\Omega}/\partial z = -i(B\langle p\rangle + C_K|\hat{\Omega}|^2\hat{\Omega}). \tag{9}$$

We have just outlined the descriptions of the pulse-medium interaction in the time domain. There is, as is well known, a fully equivalent description of this interaction in the frequency domain that is, in some instances, much more convenient to use. Therefore we now briefly summarize the description of the pulse-medium interaction in the frequency domain.[9]

We start by writing the temporal Fourier transform of the Rabi complex frequency $\hat{\Omega}(t',z)$ as

$$\tilde{\Omega}(\Delta',z) = \int_{-\infty}^{\infty}\hat{\Omega}(t',z)\exp(-i\Delta t')\,dt', \tag{10}$$

which we will occasionally represent by $\tilde{f}[\hat{\Omega}(t',z)]$. In Eq. (10) $\Delta' = \omega' - \omega_L$ are the Fourier-transform frequencies of $\hat{\Omega}(t',z)$ centered at the carrier frequency of the pulse, ω_L. Multiplying Eq. (9) by $\exp(-i\Delta' t')$ and integrating over t', we arrive at the counterpart of the Maxwell equation in the frequency domain:

$$\partial\tilde{\Omega}(\Delta',z)/\partial z = i\chi(\Delta',z)\tilde{\Omega}(\Delta',z). \tag{11}$$

We will refer to the quantity $\chi(\Delta',z)$ as the complex response function or the local susceptibility, which is given by

$$\chi(\Delta', z) = \chi'(\Delta', z) + i\chi''(\Delta', z)$$
$$= -\tilde{f}(B\langle p\rangle + C_K|\hat{\Omega}|^2|\hat{\Omega})/\tilde{\Omega}. \quad (12)$$

Equation (11) is, in most cases, a complicated nonlinear differential equation and must be solved numerically.

In analytic studies of pulse propagation in the absence of a Kerr or similar nonlinearities the concept of pulse area has proved useful.[6] The well-known McCall–Hahn area theorem describes the general features of an unchirped pulse as it propagates through a resonant medium. In order to accommodate chirping, which is always present when there is a Kerr or similar nonlinearities in the system, we generalize their concept of pulse area by establishing the definition

$$A(z) = \left|\int_{-\infty}^{\infty} \hat{\Omega}(t', z)\mathrm{d}t'\right|. \quad (13)$$

It is easy to show that $A(z) = |\tilde{\Omega}(0, z)|$, i.e., that the area of the pulse is equal to the absolute value of the Fourier transform of the pulse's complex envelope at resonance.[10]

Equation (11) with $\Delta' = 0$ and the definition in Eq. (13) lead to the equation for the space evolution of the area $A(z)$:

$$\partial A(z)/\partial z = -\chi''(0, z)A(z), \quad (14)$$

which is the analog of the equation obtained by McCall and Hahn.[6]

The differential equation for the area [Eq. (14)] can be solved analytically for weak fields where $\langle p\rangle$ is a linear function of $\tilde{\Omega}$ and $\chi(\Delta', z)$ is independent of z.[10] For strong fields it was solved by McCall and Hahn but only with $C_K = 0$, which led them to the discovery of the self-induced transparency.[6]

It can be shown (for the details see Appendix A) that for the 2π hyperbolic secant pulses the susceptibility is given by

$$\chi_0(\Delta', z) = \chi_0'(\Delta', z) = \delta\Delta', \quad (15a)$$
$$\chi_0''(\Delta', z) = 0, \quad (15b)$$

confirming that the SIT pulses are indeed energy conserving as well as shape preserving. In Eqs. (15) the subscript zero reminds us that $C_K = 0$. Moreover, the pulse delay $\delta = 1/V_s - 1/c_0$ is given by $\delta = B\tau^2\langle F(\Delta)\rangle$, where V_s is the velocity of the soliton, τ is its temporal width, and B is the propagation constant. The quantity $F(\Delta)$ is the factorization response function defined by the factorization relation

$$v(\Delta', t - z/V_s) = F(\Delta)v(0, t - z/V_s), \quad (16)$$

and $\langle F(\Delta)\rangle$ is its average over the Doppler broadening of the atomic line. In order to arrive at the above expression for δ, we used the relation $\nu_c^2\tau\langle F\rangle = 1$, established in the steady-state theory of solitons.[8] With $\chi'' = 0$ for all Δ' and with $V_s < c_0$ these pulses are truly area preserving and energy conserving.

The propagation of intense pulses in a Kerr medium is much more complex, and, as far as we know, no analytic solutions for the local susceptibility have been found in this case. In general, it must be computed numerically. However, even in this case, it is possible to obtain some useful analytic results.

Let us represent the local susceptibility in a Kerr medium by $\chi_K(\Delta', z)$. It is made up of two parts. The first part is produced by the two-level atom (TLA) resonant polarization and is given by

$$\chi_{\mathrm{TLA}}(\Delta', z) = B\tilde{f}[\langle p(\Delta, t', z)\rangle]/\tilde{\Omega}(\Delta', z). \quad (17)$$

The second part of the susceptibility $\chi_K(\Delta', z)$ is given by

$$\chi_N(\Delta', z) = C_K\tilde{f}(|\hat{\Omega}|^2\hat{\Omega})/\tilde{\Omega}(\Delta', z) \quad (18)$$

and is a result of the off-resonance polarization due to the Kerr nonlinearity. We will term it the Kerr susceptibility. Thus

$$\chi_K(\Delta', z) = \chi_{\mathrm{TLA}}(\Delta', z) + \chi_N(\Delta', z). \quad (19)$$

In general, this susceptibility must be computed numerically. However, at the beginning of the propagation, when the pulse is not yet fully coupled with the resonant and nonresonant media, we can assume that its shape is approximately the same as that of the injected pulse. Therefore $\hat{\Omega}(t, z)$ in Eqs. (17) and (18) are known quantities, and we can obtain some useful analytic results. If we make a further simplifying assumption that the initial pulse is of a hyperbolic secant shape given by $\hat{\Omega}(t', z) = (2/\tau)\mathrm{sech}(T'/\tau)$, where $T' = t' - z/V_s$, then the resonant susceptibility is given by $\chi_{\mathrm{TLA}}(\Delta', 0) = \delta\Delta'$.

The evaluation of the nonresonant susceptibility is a bit more involved. The details of this calculation are given in Appendix A, from which we quote the final results:

$$\chi_N(\Delta', 0) = C_K(2/\tau^2 + 2\Delta'^2).$$

Adding the TLA susceptibility and the nonresonant susceptibility, we obtain the total susceptibility in the presence of the Kerr nonlinearity for short propagation distances, which, after some minor algebra, can be written in the form

$$\chi_K(\Delta', 0) = \chi_K(\Delta_v', 0) + 2C_K(\Delta' - \Delta_v')^2. \quad (20)$$

Equation (20) represents a parabola in Δ' having its vertex at a point with coordinates

$$\Delta_v' = -\delta/4C_K, \quad (20a)$$
$$\chi_K(\Delta', 0) = \Delta k' + \Delta_v'\delta/2, \quad (20b)$$

where $\Delta k' = C_K\Omega_0^2/2$. This constant term $\Delta k'$, having dimensions of inverse centimeters, ought to be identified with a wave-number pulling in Eq. (4b).

The linear term in Δ' in $\chi_K(\Delta', 0)$ has its origin in $\chi_{\mathrm{TLA}}(\Delta', 0)$ and defines the SIT soliton's speed. Equation (20) is of particular importance because it is well verified by our numerical calculations (Section 3).

Finally, for short propagation distances Eq. (11) becomes

$$\partial\hat{\Omega}(\Delta', z)/\partial z = i\chi_K(\Delta', 0)\tilde{\Omega}(\Delta', z), \quad (21)$$

which can be readily solved to give

$$\tilde{\Omega}(\Delta', z) = \tilde{\Omega}(\Delta', 0)\exp\{i[\Delta k' - 4C_K\Delta_v'\Delta' + 2C_K\Delta'^2]z\}. \quad (22)$$

Taking the inverse transform of Eq. (22), we obtain the

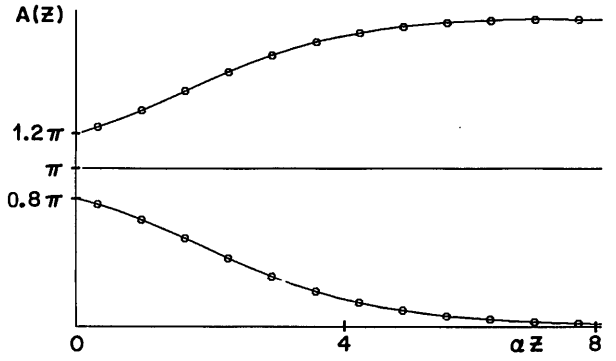

Fig. 1. Spatial evolution of the pulse area. The solid curves represent pulses in the presence of a Kerr nonlinearity, and the open circles correspond to pulses in the absence of a Kerr nonlinearity. The input pulses have Gaussian profiles with a parameterized time width $\tau = 3/2$; they are unchirped, and their initial areas are indicated. The inhomogeneous linewidth of the resonant atoms is $\tau/T_2^* = 9/2$, while the Kerr parameter of the background dielectric is $C_K = 0.01$.

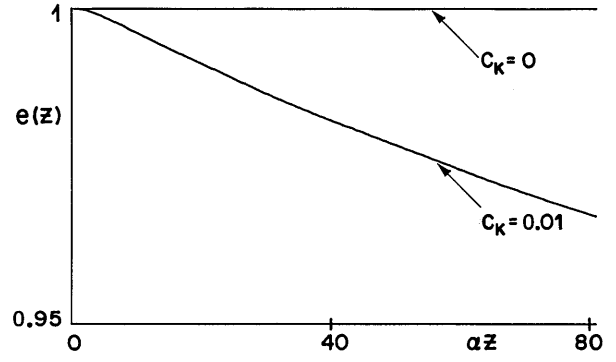

Fig. 2. Relative energy as a function of the propagation distance for a non-Kerr case ($C_K = 0$) and a Kerr case ($C_K = 0.01$) in an inhomogeneous resonant medium. The input pulses have 2π hyperbolic secant profiles with $\tau = 3/2$, and the width of the inhomogeneous line is 9/2, the same as that used in Fig. 1.

temporal description of the pulse:

$$\tilde{\Omega}(t', z) = \tilde{\Omega}_0 \frac{\sqrt{\pi}}{2} C_K z \exp\frac{i\pi}{4} \operatorname{sech}\left(\frac{t' - \delta z}{\tau}\right) \otimes \exp\left(\frac{it^2}{8C_K z}\right), \tag{23}$$

where $\otimes$ is the convolution operator.[10,12] This pulse would be area preserving and energy conserving if it could maintain the same form during the subsequent propagation. Unfortunately, we were unable to follow this propagation analytically, and therefore we had to resort to numerical calculation, the results of which we report in Section 3.[13]

3. NUMERICAL RESULTS

There are extensive numerical studies of resonant pulse propagation in Kerr-free inhomogeneous broadened media and similar systems but only a few of the case when the Kerr nonlinearity is present.[9,14] In this section we report the results of our numerical calculations on the propagation of Kerr pulses in media with broad-line resonant atoms. Our attention will focus particularly on the question of whether these pulses can attain a steady-state condition, i.e., whether they can be classified as ideal solitons.

The smallness of the Kerr constant C_K (Ref. 15) makes some numerical results uncertain, so that we do not always rely on the study of the pulse propagation in the temporal domain but also exploit the alternative description in the frequency domain in order to obtain important characteristics of these pulses. Particularly useful in this respect is the notion of local susceptibility $\chi(\Delta', z)$ introduced in Section 2. In that section it was seen how $\chi(\Delta', z)$ provides a simple and straightforward criterion for deciding whether a pulse has achieved a steady-state propagation. Only if $\chi(\Delta', z)$ is a real and linear function of Δ' is the pulse shape preserving and energy conserving, the prototype being a pure soliton of the McCall–Hahn SIT.

However, we start our investigation by solving numerically the propagation equations in the time domain [Eqs. (2)]. The initial pulses have temporal widths $\tau = 3/2$ in arbitrary units; all the other temporal and frequency units will be referred to this value.

Figure 1 shows the variation of the area $A(z)$ with the penetration distance for pulses traveling in inhomoge-

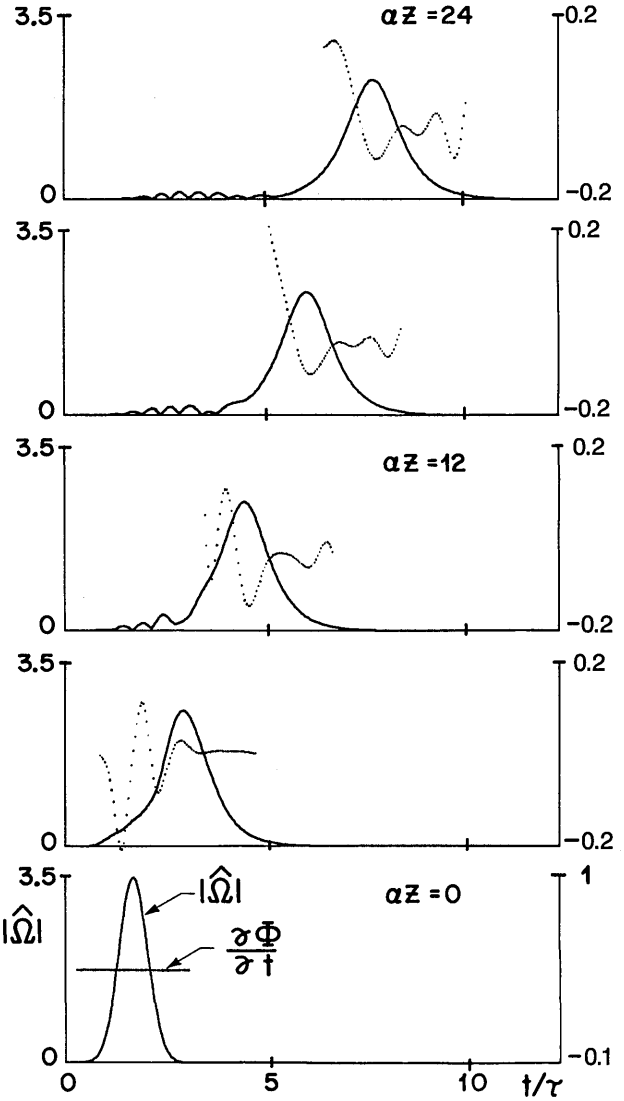

Fig. 3. Temporal behavior of the amplitude (solid curves) and the chirping (dotted curves) of the pulse as it propagates in the presence of a Kerr nonlinearity of $C_K = 0.01$. The input Gaussian pulse has an area of 1.8π, while the other parameters of this numerical simulation are the same as those used in Fig. 1.

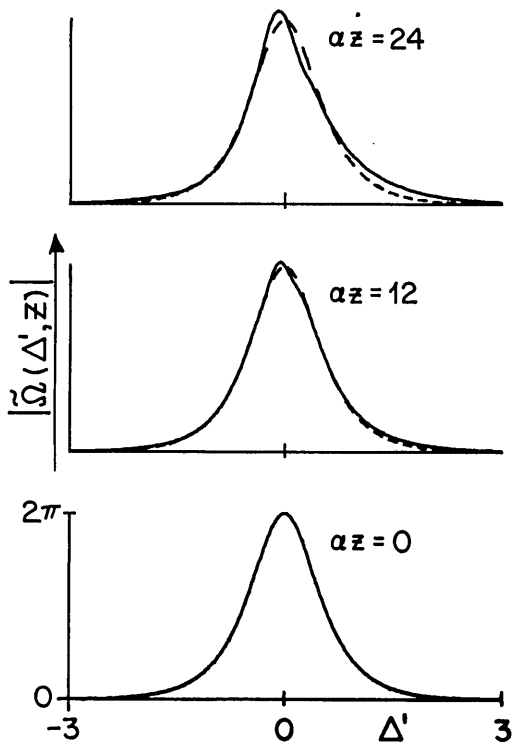

Fig. 4. Modulus of the Fourier transform of the pulse taken at three penetration distances within a resonant medium with a Kerr nonlinearity of $C_K = 0.01$. The initial 2π hyperbolic secant pulses are identical with those used in Fig. 2, but the inhomogeneous atomic line is sharp ($\tau/T_2^* = 3/20$) for the solid curve and is broad ($\tau/T_2^* = 9/2$) for the dashed curve.

neously broadened media with and without Kerr nonlinearities. The injected pulses are unchirped and have Gaussian profiles, with areas of 0.8π and 1.2π located on the 0π and 2π branches, respectively, of the McCall–Hahn area curves.[6] The area curves for the non-Kerr and Kerr cases are hardly distinguishable. In particular, the upper curves indicate that the areas of both pulses evolve toward the 2π value. It would be inappropriate to conclude, though, that the preservation of the area of the Kerr pulse implies that its energy is also conserved. That this, in fact, is not the case can be seen from Fig. 2, in which we have plotted the relative energy $e(z) = E(z)/E(0)$ for an initial hyperbolic secant pulse of area 2π entering either a Kerr medium or a Kerr-free medium. The horizontal line corresponds to the non-Kerr case and indicates that the energy of this pulse remains strictly constant. The curve corresponds to a Kerr pulse, and it clearly shows that it loses energy, although the loss is rather small, only a few percent over a considerable penetration distance of 80 Beer lengths. Here we have used 2π hyperbolic secant initial pulses in order to avoid reshaping effects that would accompany other kinds of initial pulse shapes and would mask the results of energy loss particularly at the beginning of the propagation.

The time evolution of a Gaussian pulse of Fig. 1 of initial area 1.8π is displayed in Fig. 3. Here we have plotted, as a function of time, the amplitude $|\hat{\Omega}(t',z)|$ and the chirp, computed from $\partial\Phi(t',z)/\partial t = \partial \mathrm{Im}[\ln \hat{\Omega}(t',z)]/\partial t'$, of the pulse at the entrance face of the medium and at several consecutive positions inside the medium. We see how the pulse, initially unchirped, develops an asymmetric chirp reminiscent of the chirp obtained in steady-state theory.[8] We also observe a small loss of the pulse amplitude and an increase of its width. The pulse evolves into a modulated quasi-steady-state entity with the expected reshaping process on its leading edge. Therefore the pulse in this Kerr quasi-steady-state regime is chirped, and it has a constant area but spreads out during the propagation.

We obtain further details for this quasi-steady-state pulse and the role played by the TLA's and their Doppler broadening from the frequency records of the pulse. As far as we know, no reasonable analytic approximations are available for studying the pulse behavior at large propagation distances; consequently, we explore this region nu-

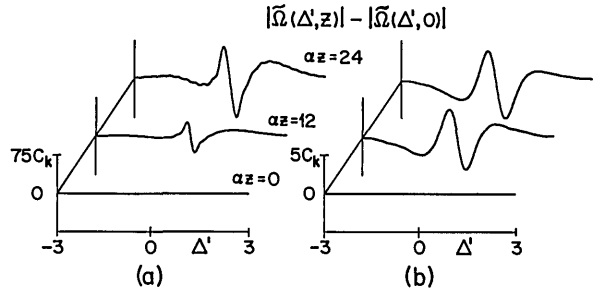

Fig. 5. Amplitude modulation of the Fourier transform of the pulses caused by the presence of a Kerr nonlinearity in the case of (a) a sharp line and (b) a broad line. The curves were obtained from Fig. 4 through the definition $\delta\tilde{\Omega} = |\tilde{\Omega}(\Delta',z)| - |\tilde{\Omega}(\Delta',0)|$ and represent the differences between the resonant propagation with and without the Kerr nonlinearity.

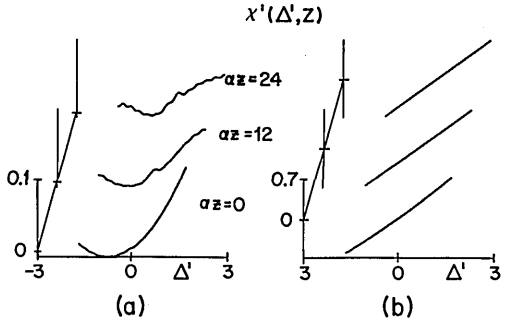

Fig. 6. Dispersive or real part of the total local susceptibility for (a) the sharp line and (b) the broad line presented in Fig. 4.

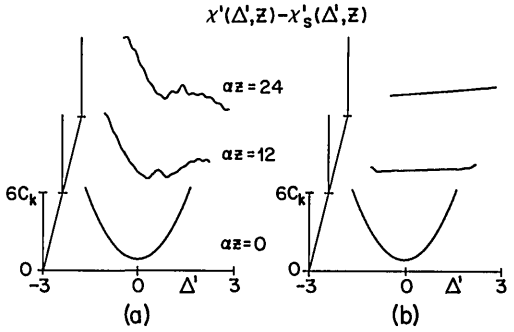

Fig. 7. Differences in the dispersive part of the local susceptibility of the resonant propagation with and without the Kerr nonlinearity for the (a) sharp-line and (b) broad-line cases. The susceptibility with the Kerr nonlinearity was taken from Fig. 6, while the Kerr-free susceptibility was obtained by the numerical solution of the propagation equations with the same parameters as those used in Fig. 4 but with $C_K = 0$.

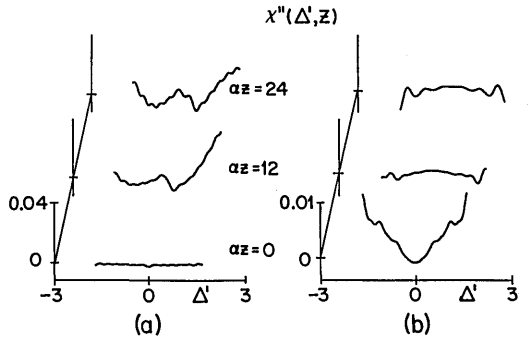

Fig. 8. Absorptive or imaginary part of the total local susceptibility for (a) the sharp line and (b) the broad line presented in Fig. 4.

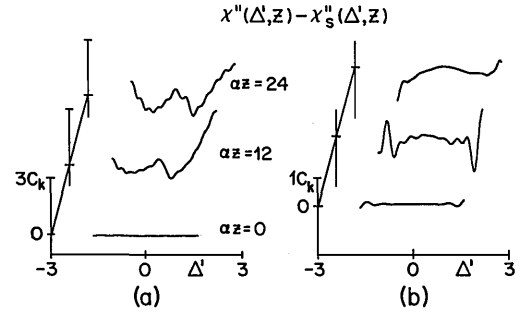

Fig. 9. Differences in the imaginary part of the local susceptibility of the resonant propagation with and without the Kerr nonlinearity for the (a) sharp-line and (b) broad-line cases. The susceptibility with the Kerr nonlinearity was taken from Fig. 7, while the Kerr-free susceptibility was obtained by the numerical solution of the propagation equations with the same parameters as those used in Fig. 4 but with $C_K = 0$.

merically, guided by the results derived in Section 2 for short propagation distances.

The influence of the Doppler broadening on the frequency distribution of the Kerr pulse is rather small, as we can see from Fig. 4, where we display the modulus of the Fourier transform of the pulse at different places in the medium.

The phase modulation is a small effect of the order of C_K, and in order to show its presence clearly we compare the Kerr pulses with the corresponding SIT solitons. There is not only a phase modulation as seen in Fig. 3 but also an amplitude modulation as is evident in Fig. 5, where we plot the difference $\partial\tilde{\Omega} = |\tilde{\Omega}(\Delta', z)| - |\tilde{\Omega}(\Delta', 0)|$ between the amplitude of the Kerr pulse, $|\tilde{\Omega}(\Delta', z)|$, and the corresponding amplitude of the soliton, $|\tilde{\Omega}(\Delta', 0)|$. This amplitude modulation strongly resembles the phase modulation at short propagation distances (see Fig. 3). The frequency pulling, the spectral narrowing, and the amplitude of the modulations are weaker for a broad line, but the spectral width of the modulation increases with the Doppler broadening.

The distinction between the lossless and linearly dispersive SIT-soliton propagation and the propagation with a loss and a dispersion introduced by a Kerr nonlinearity is best understood by an analysis of the absorptive and dispersive parts of the susceptibility. The diagrams in Figs. 6 and 7 depict the behavior of the dispersive component χ' of the susceptibility, while those in Figs. 8 and 9 show the behavior of its absorptive component χ'', for (a) a sharp atomic line and (b) a broad line. In Fig. 6(a) we see that for the narrow line the parabolic dispersion (quadratic dependence on Δ') at short propagation distance, which we predicted in Section 2, progressively changes into a linear one.

We trace the origin of the energy loss by the pulse to its interaction with the dipoles of the TLA's, specifically to the behavior of their absorptive components $v(\Delta, t', z)$, which are individualized by their detunings Δ. It is well known that, in the absence of the Kerr nonlinearity, the temporal behavior of individual v's is antisymmetric in time and that all of them are in phase in the sense that all pass through zero at the same time and achieve their local extremes simultaneously, tracing curves of similar shapes. Moreover, the curves for a detuning Δ and the opposite detuning $-\Delta$ coincide [see Fig. 10(a)]. This behavior persists along the whole propagation distance; the results in

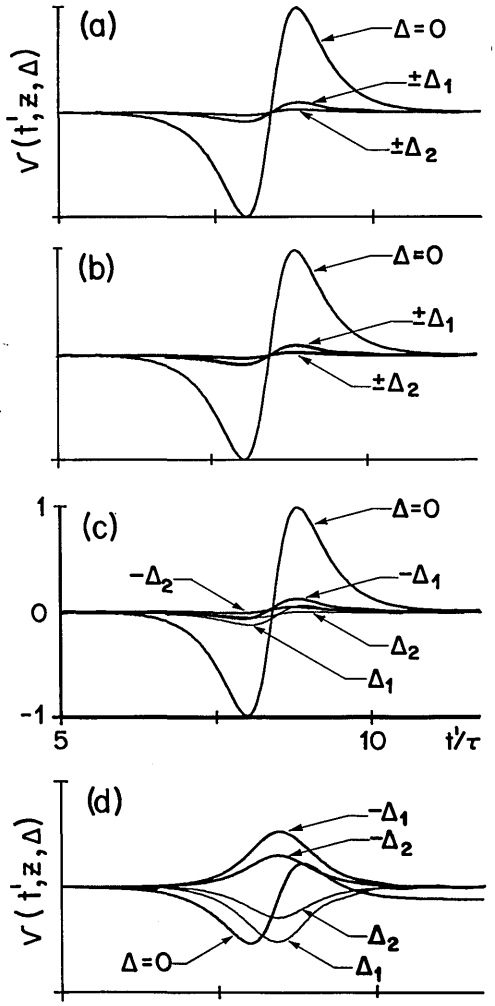

Fig. 10. Temporal dephasing introduced by the Kerr nonlinearity in the individual behavior of the absorptive part of the atomic polarization, $v(t', z, \Delta)$. The case in (a) corresponds to the Kerr-free medium. The curves of TLA's for different detunings follow, but for a scale factor, the same time evolution. We also note that a TLA of detuning Δ follows exactly the behavior exhibited by a TLA with detuning $-\Delta$, permitting the factorization of u. The presence of the Kerr nonlinearity introduces both the dephasing and the asymmetry of the temporal behavior of v and inhibits the factorization. All the curves are obtained at a propagation distance $\alpha z = 24$ within the medium and under circumstances identical to those used in Fig. 2. In (b) $C_K = 0.0001$, in (c) $C_K = 0.001$, and in (d) $C_K = 0.01$. Same scale for (a)–(d).

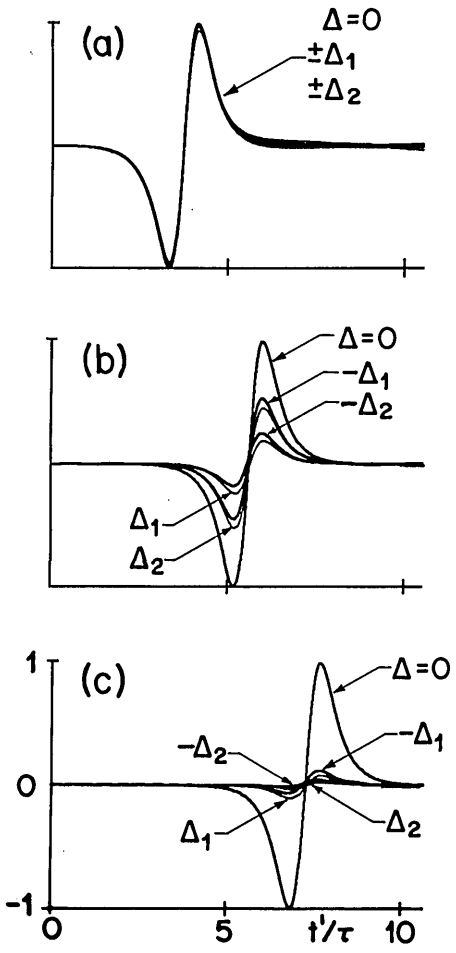

Fig. 11. Influence of the Doppler broadening on the temporal behavior of $v(t', z, \Delta)$ during the resonant propagation in the presence of the Kerr nonlinearity ($C_K = 0.001$). The sharp-line case, shown in (a), corresponds to the analytic solution of Ref. 5. When the Doppler width is increased, the effects of dephasing and asymmetry on v become evident. The curves are taken at the propagation distance $\alpha z = 24$ and under the circumstances described in Fig. 2. In (a) $\tau/T_2^* = 3/20$, in (b) $\tau/T_2^* = 3/2$, and in (c) $\tau/T_2^* = 9/2$. Same scale for (a)–(c).

Fig. 10 correspond to a large propagation distance of $\alpha z = 24$, where we suspect that the steady-state conditions are achieved. It is this behavior of the dipoles of the TLA's that permits us to write $v(\Delta, t', z) = F(\Delta)v(0, t', z)$; that is to say, this particular behavior is the source of the all-important factorization assumption. Therefore this assumption is not a pure mathematical ansatz, useful in obtaining analytic solutions, but has a firm basis in the physical behavior of the resonant atoms.

Numerical solutions for an input 2π hyperbolic secant pulse show that, as the Kerr nonlinearity is increased within its allowed perturbative range, the behavior of $v(\Delta', z, t)$ changes drastically. This is seen in Figs. 10(b), 10(c), and 10(d), where the Kerr constant C_K assumes the values 0.0001, 0.001, and 0.01, respectively. For $C_K = 0.0001$ the change is not noticeable at the scale of the drawing, but for $C_K = 0.001$ and $C_K = 0.01$ it is obvious. We see that only the curves for on-resonance atoms ($\Delta' = 0$) pass through the origin, while the curves of all other atoms cross the time axis at progressively larger times. We see also that the curves for $\pm\Delta$ are now separated.

Not only is this distortion dependent on the magnitude of the Kerr nonlinearity itself but it also strongly depends on the value of the inhomogeneous broadening. The diagrams in Fig. 11 show this effect nicely. When the line is narrow ($\tau/T_2^* = 0.15$), the curves for $v(\Delta', t', z)$ almost coincide, but as τ/T_2^* increases, these curves grow more and more out of step. It is now clear why all previous attempts to obtain analytic solutions for the steady-state equations of motion in the presence of the Kerr nonlinearity in inhomogeneous absorbers by using the factorization assumption have failed. They have failed because the factorization assumption itself fails; i.e., the function F in $v(\Delta, t', z) = F(\Delta)v(0, t', z)$ is itself, in this case, a function of time.

4. CONCLUSIONS

The present numerical studies have shown, contrary to our expectations,[8] that an absorber composed of inhomogeneously broadened two-level atoms embedded in a nonlinear Kerr host dielectric cannot support propagation of an ideal soliton. We have found, in fact, that a pulse propagating through such a medium loses its energy, although it seems to maintain its area. However, this energy loss is so small, even along a considerable propagation distance, that it will be difficult to distinguish these Kerr pulses from true solitons in a laboratory experiment in which, in any case, the transverse effects limit the coherent propagation to some 10 Beer lengths. For this reason we call these pulses quasi-stationary. We have demonstrated the energy degradation of these pulses through their space evolution as well as through the analysis of the local susceptibility in the frequency domain. We have found that the physical reason for the energy loss of the pulse is the asymmetry, introduced by the Kerr nonlinearity, in the temporal evolution of the absorptive components of the resonant atoms. This microscopic effect invalidates the so-called factorization assumption, while its macroscopic average results in a barely detectable loss of the pulse's energy.

APPENDIX A: DERIVATIONS OF EQS. (20)

We start with Eq. (12) in the text for the case $C_K = 0$ and where $\tilde{\Omega}(\Delta', z)$ is the Fourier transform of the McCall–Hahn soliton $\tilde{\Omega}(t', z) = \Omega_0 \operatorname{sech}(T'/\tau)$ ($\Omega_0 = 2/\tau, T' = t' - z/V_s$). Hence

$$\tilde{\Omega} = \int_{-\infty}^{\infty} \exp(i\Delta' t')\,(2/\tau)\operatorname{sech}(T'/\tau)\,dt'$$

$$= 2\pi \operatorname{sech}(\pi\tau/2). \tag{A1}$$

Next, we compute

$$\tilde{f}(B\langle p\rangle) = B\tilde{f}(\langle u\rangle + i\langle v\rangle).$$

The first term vanishes because $u(\Delta, t')$ is odd in t' and because we are taking $g(\Delta')$ to be an even function of Δ' (Gaussian). The second term can be written as

$$\tilde{f}(iB\langle v\rangle) = 2iB\langle F\rangle \int_{-\infty}^{\infty} \exp(i\Delta' t')\operatorname{sech}(T'/\tau)\tanh(T'/\tau)\,dt'$$

$$= -2iB\tau\langle F\rangle \int_{-\infty}^{\infty} \exp(i\Delta' t')[\operatorname{sech}(T'/\tau)/\partial t']\,dt';$$

when the known properties of Fourier transform for the derivatives are used, the preceding equation reduces to

$$\tilde{f}(iB\langle v\rangle) = -2B\pi\tau^2\langle F\rangle\Delta' \operatorname{sech}(\pi\tau\Delta'/2).$$

Hence the susceptibility due to TLA's can be written as

$$\chi_{\mathrm{TLA}}(\Delta', z) = \delta\Delta'. \tag{A2}$$

In deriving Eq. (A1) we have used the steady-state relation[8]

$$\nu_c^2\tau^2\langle F\rangle = 1. \tag{A3}$$

The simplest way of establishing this relation is to start with the steady-state equation for Ω and use the factorization assumption:

$$\Omega = \nu_c^2\langle F\rangle v(0, t'). \tag{A4}$$

On the other hand, the derivative of the hyperbolic secant soliton permits us to write

$$\Omega = -(1/\tau^2)v(0, t'). \tag{A5}$$

Equating the right-hand sides of Eqs. (A4) and (A5), we obtain Eq. (A3).

Now we must calculate the nonresonant susceptibility

$$\chi_N(\Delta', z) = C_K\tilde{f}(|\hat{\Omega}|^2\hat{\Omega})/\tilde{\Omega}, \tag{A6}$$

where $\tilde{\Omega}$ is given by Eq. (A1). The Fourier transform in the numerator in Eq. (A6) can be written as

$$\tilde{f}(|\hat{\Omega}|^2\hat{\Omega}) = \frac{8}{\tau^3}\int_{-\infty}^{\infty} \exp(i\Delta t')\operatorname{sech}^3(T'/\tau)\mathrm{d}t'.$$

We can find the Fourier transform of $\operatorname{sech}^3(T'/\tau)$ in Ref. 16, which leads to

$$\tilde{f}(|\hat{\Omega}|^2\hat{\Omega}) = 4\pi(1/\tau^2 + \Delta'^2)\operatorname{sech}(\pi\tau\Delta'/2). \tag{A7}$$

Substitution of Eqs. (A1) and (A7) into Eq. (A6) leads to the result in the text.

Finally, the total Kerr susceptibility at the beginning of the propagation,

$$\chi_K(\Delta', 0) = \delta\Delta' + C_K(\Omega_0^2/2 + 2\Delta'^2),$$

can be rewritten, by the technique of completing the square in the second term, as

$$\chi_K(\Delta', 0) = C_K\Omega_0^2/2 + \delta\Delta_v'/2 + 2C_K(\Delta' + \delta/4C_K)^2,$$

where $\Delta_v' = \delta/C_K$. Since $\chi_K(\Delta_v', 0) = C_K\Omega^2/2 + \delta\Delta_v'/2$, we obtain Eqs. (20) of Section 2.

ACKNOWLEDGMENT

The first author is indebted to C. Palmer for several valuable comments.

*Permanent address, Department of Physics, St. John Fisher College, Rochester, New York 14618.

†Permanent address, Coordinación Académica, Grupo Educativo Ima, Apartado Postal 172, Cortazar, Quanajuato, México 38301.

REFERENCES AND NOTES

1. A. Hasegawa and F. Tappert, Appl. Phys. Lett. **233,** 142 (1973); Appl. Phys. Lett. **239,** 142 (1973).
2. W. H. Knox, R. L. Fork, M. C. Downer, R. H. Stolen, J. A. Valmanis, and C. V. Shank, Appl. Phys. Lett. **46,** 1120 (1985); R. L. Fork, C. H. Brito Cruz, P. C. Becker, and S. V. Shank, Opt. Lett. **12,** 483 (1987).
3. R. H. Stolen, L. F. Mollenauer, and W. J. Tomlinson, Opt. Lett. **83,** 186 (1988).
4. J. H. Eberly and L. Matulic, Opt. Commun. **1,** 241 (1969).
5. L. Matulic and J. H. Eberly, Phys. Rev. A **6,** 882 (1972).
6. S. L. McCall and E. L. Hahn, Phys. Rev. **183,** 457 (1969).
7. R. Michalska-Trautman, Phys. Rev. A **17,** 176 (1978).
8. L. Matulic, C. Palmer, J. J. Sánchez-Mondragón, and G. E. Torres-Cisneros, J. Opt. Soc. Am. B **5,** 1673 (1988).
9. L. Matulic, G. E. Torres-Cisneros, and J. J. Sánchez-Mondragón, in *Optical Society of America Annual Meeting,* Vol. 18 of 1989 OSA Technical Digest Series (Optical Society of America, Washington, D.C., 1989), p. 241.
10. L. Matulic, J. J. Sánchez-Mondragón, G. E. Torres-Cisneros, and E. Chávez-Cortés, Rev. Mex. Fis. **31,** 259 (1985).
11. F. A. Hopf and M. O. Scully, presented at the Conference on Physics and Quantum Electronics, Prescott, Ariz., 1970.
12. For more details about the topics treated in Section 2 the reader may consult D. C. Champeney, *Fourier Transforms and Their Physical Applications* (Academic, London, 1973).
13. E. L. Gieszelman, Tech. Rep. 80, Optical Sciences Center (University of Arizona, Tucson, Ariz., 1973).
14. O. Barbosa-Garcia, G. E. Torres-Cisneros, and J. J. Sánchez-Mondragón, Opt. Lett. **13,** 999 (1988).
15. Taking, for instance, the value of the Kerr constant β for glass as given by R. Y. Chio, F. Garmire, and C. H. Townes, Phys. Rev. Lett. **13,** 479 (1964), we find that $C_K \approx 2.5 \times 10^{-2}\ \mathrm{cm^{-1}\ s^{-2}}$.
16. F. Oberhettinger, *Fourier Transforms of Distributions and Their Inverses* (Academic, New York, 1973), p. 36, item 179.